JOURNAL OF SPACECRAFT AND ROCKETS
Vol. 55, No. 4, July–August 2018

Engineering Notes

Numerical Evaluation of Post-Newtonian Perturbations on the Global Navigation Satellite System

Kyoung-Min Roh*
Korea Astronomy and Space Science Institute, Daejeon 34055, Republic of Korea

DOI: 10.2514/1.A33980

I. Introduction

PRECISE orbital knowledge is one of the most stringent requirements for a global navigation satellite system (GNSS) because the positions of the GNSS satellites serve as reference points. If the reference points are provided with high precision, better solutions can be achieved in most applications, such as positioning and time synchronization. One of the most important issues for precise orbit determination is that the orbital dynamic model should have an accuracy equivalent to that of the measurements. The measurement technology of the GNSS, based on the time and frequency transfer through atomic clocks, has achieved an accuracy on the order of 1×10^{-16}, which is several orders of magnitude lower than that of the relativistic effect. The continuing progress in atomic clocks is expected to improve the accuracy at the rate of one order of magnitude per decade. There have been several extensive studies about the relativistic effects on the signal and time transfer in the GNSS [1]. The major relativistic effect of gravitational blue shift has already been taken into account in the Global Positioning System (GPS). The clocks on GPS satellites are adjusted so that the clocks appear to a ground station to have its chosen frequency. The details and additional relativistic effects on the atomic clocks in the GNSS satellites will not be discussed here because this Note focuses on the relativistic effects on the equations of motion of the GNSS satellites. Readers interested in the relativistic effects on the atomic clocks in the GNSS satellites can refer to the paper by Ashby [2].

According to the advances in measurement systems, the dynamic model (i.e., the equations of motion of satellites) also needs to take into account the relativistic effects. Therefore, the International Earth Rotation and Reference System Service (IERS) has first recommended that the largest relativistic effect must be included (i.e., the Schwarzschild terms), and this recommendation appeared in the IERS standards of 1992 [3]. The latest IERS conventions of 2010 [4] suggested that two additional relativistic perturbations (i.e., the Lense–Thirring effect and de Sitter precession) should be taken into account for precise orbit determination. However, these two additional relativistic terms are still often ignored in GPS data processing [5].

These relativistic perturbations are derived from the post-Newtonian (PN) approximation of a metric tensor defined with respect to the Earth's center, namely, the geocentric metric tensor. These approximated equations of motion can be described as a sum of the Newtonian term and the PN corrections. The aforementioned three PN corrections, or perturbations, are calculated by assuming the Earth has a spherical-symmetric gravitational field and a constant rotation rate. However, there are other PN perturbations caused by the nonsymmetrical shape of our planet and the PN tidal gravitational potential owing to the external bodies in our solar system. These additional PN corrections have not been considered yet because they are estimated to be minute as compared with other perturbations, such as due to the radiation pressures due to the sun and the Earth [6]. Advanced perturbation models and measurement technology (i.e., atomic clocks) prompt the investigation of the impact of previously ignored PN corrections. Even small errors in attitude or rigid-body models of spacecraft can affect the satellite's orbit determination results [7]. Therefore, it is important to evaluate the impact of PN corrections by conducting comprehensive numerical simulations; the results are likely to be very useful for defining the accuracy of the orbital dynamic models of the GNSS orbit for precise orbit determination.

Our main motivation in this work was to investigate the effects of the full set of first-order PN perturbations on the GNSS orbits, specifically on the GPS and the Russia's global navigation satellite system (GLONASS) orbits. There were also several other satellite navigation systems, such as BeiDou (People's Republic of China), Galileo (European Union), and the Quasi-Zenith Satellite System (Japan). However, these systems were not studied here because they are not yet fully operational. The full set of first-order PN corrections was first implemented by Roh et al. [8] in the high-fidelity orbit propagation software KASIOP (which stands for Korea Astronomy and Space Science Institute Orbit Propagator), and their effects on orbital elements were numerically evaluated for the laser geodynamics satellite (LAGEOS) and laser relativity satellite (LARES) orbits. The details about KASIOP can be found in [8]. The LAGEOS-1 and -2 missions provided the first experimental results for the Lense–Thirring effect, which is also known as the frame-dragging effect. The LARES satellite was launched in 2012 to measure the frame-dragging effect with an accuracy of ∼1% [9]. However, these satellites have a small cannonball-shaped spacecraft with a low area-to-mass ratio to reduce any nonconservative perturbations such as atmospheric drag and radiation pressure from the sun and the Earth. The properties of the GPS and the GLONASS spacecraft are quite different from those of the LAGEOS and the LARES systems in many aspects, such as their box-wing shape, large solar panels, and semimajor axes of ∼26, 000 km, which are nearly twice that of the LAGEOS system. In this Note, the full first-order PN corrections were numerically simulated and investigated for the GPS and the GLONASS cases using the software that was previously developed by Roh et al. [8].

The PN equations of motion studied in this work are briefly introduced in Sec. II, and the details of the numerical simulations and the results are presented in Sec. III. Lastly, the summary and concluding remarks are presented in Sec. IV.

II. Background and Simulation Scope

A. Post-Newtonian Equations of Motion

The general theory of relativity (GR) deals with gravity. The space–time around a body with a certain mass is curved, and gravity can be thought of as a curvature of space–time in the GR. Namely, the geometry of space–time, described mathematically using a metric tensor, defines the motion of a particle in the space–time continuum. Resolution B1.3 of 2000 [10] adopted by the International Astronomical Union (IAU) states the relativistic reference frames based on the metric tensors defined for the geocentric and barycentric

Received 18 May 2017; revision received 26 December 2017; accepted for publication 7 January 2018; published online 27 February 2018.

*Senior Research Staff, Space Science; kmroh@kasi.re.kr.

coordinates, i.e., the geocentric celestial reference system (GCRS) and the barycentric celestial reference system. The formulas in Resolution B1.3 of 2000 are based on the studies done by two groups, namely, Brumberg and Kopejkin [11] and Damour et al. [12–15]. In the studies, the geocentric reference frame was defined in the framework of the GR and the geocentric metric tensor was derived by matching the barycentric and geocentric metrics approximated up to the first-order PN terms in the overlapping region of the two metrics. Using the derived geocentric metric tensor, the PN equations of motion of a near-Earth satellite could be formulated using the geodesic equation of motion. The formulas derived by Brumberg and Kopejkin [11] were used in this study. The resultant equations of motion are

$$\frac{\mathrm{d}^2\boldsymbol{r}}{\mathrm{d}t^2} = \boldsymbol{a}_N + \boldsymbol{a}_{\mathrm{NC}} + \frac{1}{c^2}\sum_{i=1}^{7}\boldsymbol{\Phi}_i \tag{1}$$

where $(\boldsymbol{r}, t)$ is the geocentric coordinate and time, $\boldsymbol{a}_N$ is the Newtonian acceleration vector, $\boldsymbol{a}_{\mathrm{NC}}$ is the acceleration due to nonconservative forces (such as the radiation pressures from the sun and the Earth), and $\boldsymbol{\Phi}_i$ are the first-order PN perturbations. In this Note, the first-order PN perturbations $\boldsymbol{\Phi}_i$, were divided into seven accelerations. The PN corrections from $\boldsymbol{\Phi}_1$ to $\boldsymbol{\Phi}_6$ refer to the same terms in [8], in which the exact expressions for $\boldsymbol{\Phi}_i$ can be found. Specifically, $\boldsymbol{\Phi}_i$ contain the relativistic Schwarzschild perturbation owing to a spherically symmetric component of the geopotential ($\boldsymbol{\Phi}_1$), the Lense–Thirring force due to the Earth's constant rotation ($\boldsymbol{\Phi}_2$), the relativistic effect owing to the Earth's quadrupole moment ($\boldsymbol{\Phi}_3$), a nonlinear coupling of the monopole attracting force of the Earth and the gravitoelectric tidal field of the solar system bodies ($\boldsymbol{\Phi}_4$), and gravitomagnetic and gravitoelectric components of the tidal perturbations ($\boldsymbol{\Phi}_5$, $\boldsymbol{\Phi}_6$). The last PN correction, $\boldsymbol{\Phi}_7$, is the geodesic precession also known as "de Sitter precession," which corresponds to an acceleration that is added to compensate for the slow PN precession of the spatial axes of the geocentric frame with respect to the barycentric one in order to keep the "kinematically nonrotating" definition of the GCRS [10]. The $\boldsymbol{\Phi}_1$, $\boldsymbol{\Phi}_2$, and $\boldsymbol{\Phi}_7$ terms are accelerations that the IERS Conventions of 2010 [4] suggested for inclusion in all high-precision orbit calculations. In this study, all other relativistic perturbations were taken into account for the GPS and the GLONASS orbits, as well as the IERS-mentioned three terms.

B. Numerical Simulations

The numerical simulations of the effect of these first-order PN corrections are conducted for the GPS and the GLONASS systems because they are the representative operational GNSS orbits. These two orbits have similar orbital properties, i.e., their altitudes are ~20,000 km and their inclinations are medium. Therefore, in this study, five orbits are selected with different ascending nodes and different body types. The orbital elements and the body models of the studied satellites in here are summarized in Table 1. The values in Table 1 are the osculating orbital elements calculated from the final orbit solution released by the International GNSS Service (IGS) for 1 January 2006.

The magnitudes of the first-order PN corrections are very small; therefore, high-precision orbit propagation software should be used for realistic simulations. Here, we use the KASIOP package that was developed by the Korea Astronomy and Space Science Institute; this orbit propagator was also used and validated previously when studying the effects of the PN corrections on the LARES orbit [8]. Therefore, in what follows, we only describe the most important aspects of the implementation process of the full set of first-order PN corrections. The reference coordinates and time for the numerical integration of the equations of motion of the studied satellites are set to the Earth-centered International Celestial Reference System, which is also known as J2000.0 and terrestrial time, respectively. Therefore, the coordinate and time transformations were conducted before and after the calculations of the PN terns because the relativistic perturbations were derived in the relativistic reference system, i.e., the GCRS and the Geocentric Coordinate Time, respectively. Note also that the relativistic correction owing to the Earth's quadrupole moment (i.e., $\boldsymbol{\Phi}_3$,) was calculated by taking into account only the J2 term. The included perturbations and space environment models, as well as the numerical methods such as integration and interpolation, are listed in Table 2 [7,16–20]. The only difference from the previous study is the calculation of the perturbation due to the radiation pressure. The spacecraft bodies of the GPS and the GLONASS are modeled as box-wing shaped, unlike the cannonball-shaped LAGEOS system. Therefore, the perturbations due to the sun- and Earth-related radiations were calculated by taking into account the spacecraft-specific body model and nominal attitude. The details of the implementation process of the first-order PN corrections and the orbit propagation software can be found in [8].

Table 2 Lists of the models applied to the orbit propagation

Item	Applied model
Geopotential	Earth Gravitational Model 2008, 70×70
Zero-tide geopotential	IERS Conventions of 2010 [4]
Solid Earth/solid Earth pole/ ocean pole tide	[16]
Ocean tide	Finite element solution 2004 [17]
Earth rotation	
Precession-nutation	IAU 2006/2000
Earth rotation parameters	IERS ERP C04
Numerical method	10th-order summed Adams–Bashforth–Moulton [18]
Integration	60s of the step size
Interpolation	10th-order Lagrangian
Space environments	JB2008 [19]
Atmospheric density	Rodrigues–Solano et al. [7]
Earth radiation	INPOP 13c [20]
Solar system ephemeris	
Spacecraft body Box-wing model	Rodrigues–Solano et al. [7]

III. Simulation Results

The orbit propagation results for the GPS and GLONASS with the PN corrections are presented in this section. First, the magnitudes of the different PN terms were investigated for one of the GPS satellites, PRN01, because the orbital properties of the two systems (GPS and GLONASS) were similar, except for the ascending node,

Table 1 Orbital elements and body types of the tested GNSS satellites

	GPS-01	GPS-02	GPS-05	GLONASS-01	GLONASS-25
Body model	BLOCK IIF	BLOCK IIR-B	BLOCK IIR-M	GLONASS-M	GLONASS-K1
a, km	26558.614	26559.232	26562.4368	25506.554	25509.582
e	0.0049339050	0.0152212291	0.0046427301	0.0004006854	0.0007265757
i, deg	55.289	54.073	54.198	64.128	65.258
Ω, deg	121.702	119.395	180.865	201.5904	82.512
ω, deg	27.344	234.448	27.744	26.489	218.694

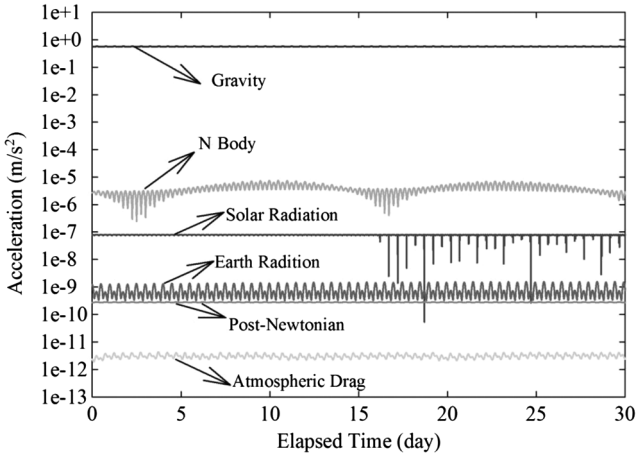

Fig. 1 Accelerations of GPS PRN01.

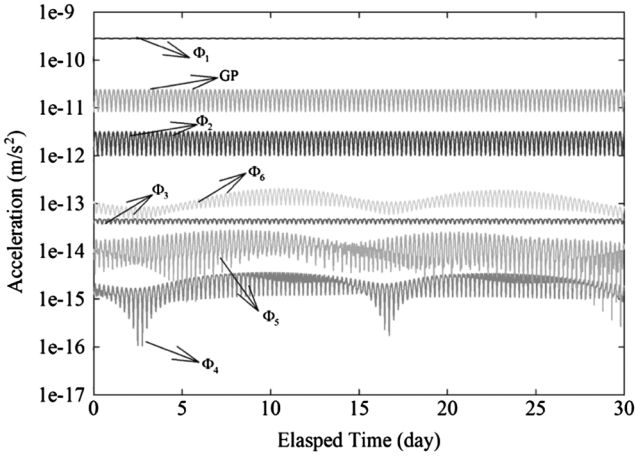

Fig. 2 Accelerations of the PN corrections for GPS PRN01.

as shown in Table 1. The total sum of all PN corrections is plotted in Fig. 1 for one month of orbit propagation, along with all the other perturbations applied in this study. The accelerations associated with the different PN corrections are plotted in Fig. 2. Figure 1 shows that the accelerations, in descending order of their overall magnitude, are as follows: perturbations owing to the nonsymmetric geopotential, third bodies, solar radiation, Earth's radiation, PN terms, and (lastly) atmospheric drag. The spikes in the solar radiation force are caused by eclipses. The PN perturbations are on the order of 3×10^{-10} m/s^2, which is a couple of orders lower than the perturbations for the low Earth orbit, such as that of the LARES system [8]. The reason for this lower value is that the semimajor axis of the GPS orbit is much larger than that of the LARES, i.e., 7820 km. Namely, the Schwarzschild perturbation, which is the largest contribution and caused by a spherically symmetric part of the geopotential, is proportional to the distance from the Earth's center. Next, contributions come from $\mathbf{\Phi}_7$ (denoted by GP), $\mathbf{\Phi}_2$, $\mathbf{\Phi}_6$, $\mathbf{\Phi}_3$, $\mathbf{\Phi}_5$, and $\mathbf{\Phi}_4$. The largest three terms are the perturbations recommended by the IERS Conventions of 2010 [4]. In Fig. 2, the gravitoelectric component of the tidal perturbation $\mathbf{\Phi}_6$, is larger than the relativistic correction due to the Earth's quadrupole moment $\mathbf{\Phi}_3$, which is the largest relativistic acceleration in the LAGEOS and LARES cases, except the three terms listed in the IERS Conventions [8]. However, this phenomenon can also be understood by considering that the altitude of the GPS orbit is about twice as high as the LAGEOS orbit. Namely, the GPS orbit is more sensitive to the tidal potential than the relativistic corrections due to the nonsymmetric geopotential. The long-term variations of $\mathbf{\Phi}_4$ to $\mathbf{\Phi}_6$ are related to the tidal potential caused by the external bodies in our solar system. The properties of the decomposed accelerations for all the PN corrections have been previously analyzed by Roh et al. [8]. Therefore, the decomposed accelerations into radial/alongtrack/crosstrack components for the GPS orbit simulated in this study are listed in the Appendix.

Figure 3 shows the simulation results for the five satellites, specifically, GPS PRN02 (G02), GPS PRN05 (G05), GLONASS PRN01 (R01), and GLONASS PRN26 (R26), in addition to GPS PRN01 (G01). Only the accelerations of $\mathbf{\Phi}_3$, $\mathbf{\Phi}_4$, $\mathbf{\Phi}_5$, and $\mathbf{\Phi}_6$ are displayed because the other three terms (i.e., $\mathbf{\Phi}_1$, $\mathbf{\Phi}_2$, and $\mathbf{\Phi}_7$) are relatively well known. The x-axis in Fig. 3 is the argument of latitude (i.e., the sum of the argument of perigee and true anomaly) in order to monitor changes in the acceleration as a function of the orbital position for one orbit. The $\mathbf{\Phi}_3$ accelerations in Fig. 3a due to the relativistic effect of the Earth's quadrupole moments can be divided into two groups (i.e., the GPS and the GLONASS), and this phenomenon is mainly caused by the semimajor axis difference. The other three terms, related to the tidal potential, can be divided into three groups, i.e., (G01, G02), (G05, R01), and (R26), as shown in Figs. 3b–3d. These three groups are related to their orbital planes, as can be seen from the ascending nodes in Table 1, because the tidal potential is directly related to their orbital planes.

Lastly, the effects of the PN corrections on satellite orbits were analyzed by comparing two orbits with and without a specific PN term. The seven cases are listed according to the magnitudes of the PN corrections, and the maximal positional differences in radial/alongtrack/crosstrack components are calculated for the following cases:

Case 1:

$$(a_N + a_{\mathrm{NC}} + \mathbf{\Phi}_1) - (a_N + a_{\mathrm{NC}})$$

Case 2:

$$(a_N + a_{\mathrm{NC}} + \mathbf{\Phi}_1 + \mathbf{\Phi}_{\mathrm{GP}}) - (a_N + a_{\mathrm{NC}} + \mathbf{\Phi}_1)$$

Case 3:

$$(a_N + a_{\mathrm{NC}} + \mathbf{\Phi}_1 + \mathbf{\Phi}_{\mathrm{GP}} + \mathbf{\Phi}_2) - (a_N + a_{\mathrm{NC}} + \mathbf{\Phi}_1 + \mathbf{\Phi}_{\mathrm{GP}})$$

Case 4:

$$(a_N + a_{\mathrm{NC}} + \mathbf{\Phi}_1 + \mathbf{\Phi}_{\mathrm{GP}} + \mathbf{\Phi}_2 + \mathbf{\Phi}_6) - (a_N + a_{\mathrm{NC}} + \mathbf{\Phi}_1 + \mathbf{\Phi}_{\mathrm{GP}} + \mathbf{\Phi}_2)$$

Case 5:

$$(a_N + a_{\mathrm{NC}} + \mathbf{\Phi}_1 + \mathbf{\Phi}_{\mathrm{GP}} + \mathbf{\Phi}_2 + \mathbf{\Phi}_6 + \mathbf{\Phi}_3) - (a_N + a_{\mathrm{NC}} + \mathbf{\Phi}_1 + \mathbf{\Phi}_{\mathrm{GP}} + \mathbf{\Phi}_2 + \mathbf{\Phi}_6)$$

Case 6:

$$(a_N + a_{\mathrm{NC}} + \mathbf{\Phi}_1 + \mathbf{\Phi}_{\mathrm{GP}} + \mathbf{\Phi}_2 + \mathbf{\Phi}_6 + \mathbf{\Phi}_3 + \mathbf{\Phi}_5) - (a_N + a_{\mathrm{NC}} + \mathbf{\Phi}_1 + \mathbf{\Phi}_{\mathrm{GP}} + \mathbf{\Phi}_2 + \mathbf{\Phi}_6 + \mathbf{\Phi}_3)$$

Case 7:

$$(a_N + a_{\mathrm{NC}} + \mathbf{\Phi}_1 + \mathbf{\Phi}_{\mathrm{GP}} + \mathbf{\Phi}_2 + \mathbf{\Phi}_6 + \mathbf{\Phi}_3 + \mathbf{\Phi}_5 + \mathbf{\Phi}_4) - \left(a_N + a_{\mathrm{NC}} + \sum_{i=1}^{7} \mathbf{\Phi}_i\right)$$

By performing this test, we estimated the effects of specific PN terms as well as the cumulative effect. In what follows, we only integrated the equations for GPS PRN01 for one week, for the same time window as in previous tests, and the results are summarized in Table 3. The GLONASS case was not considered here because the

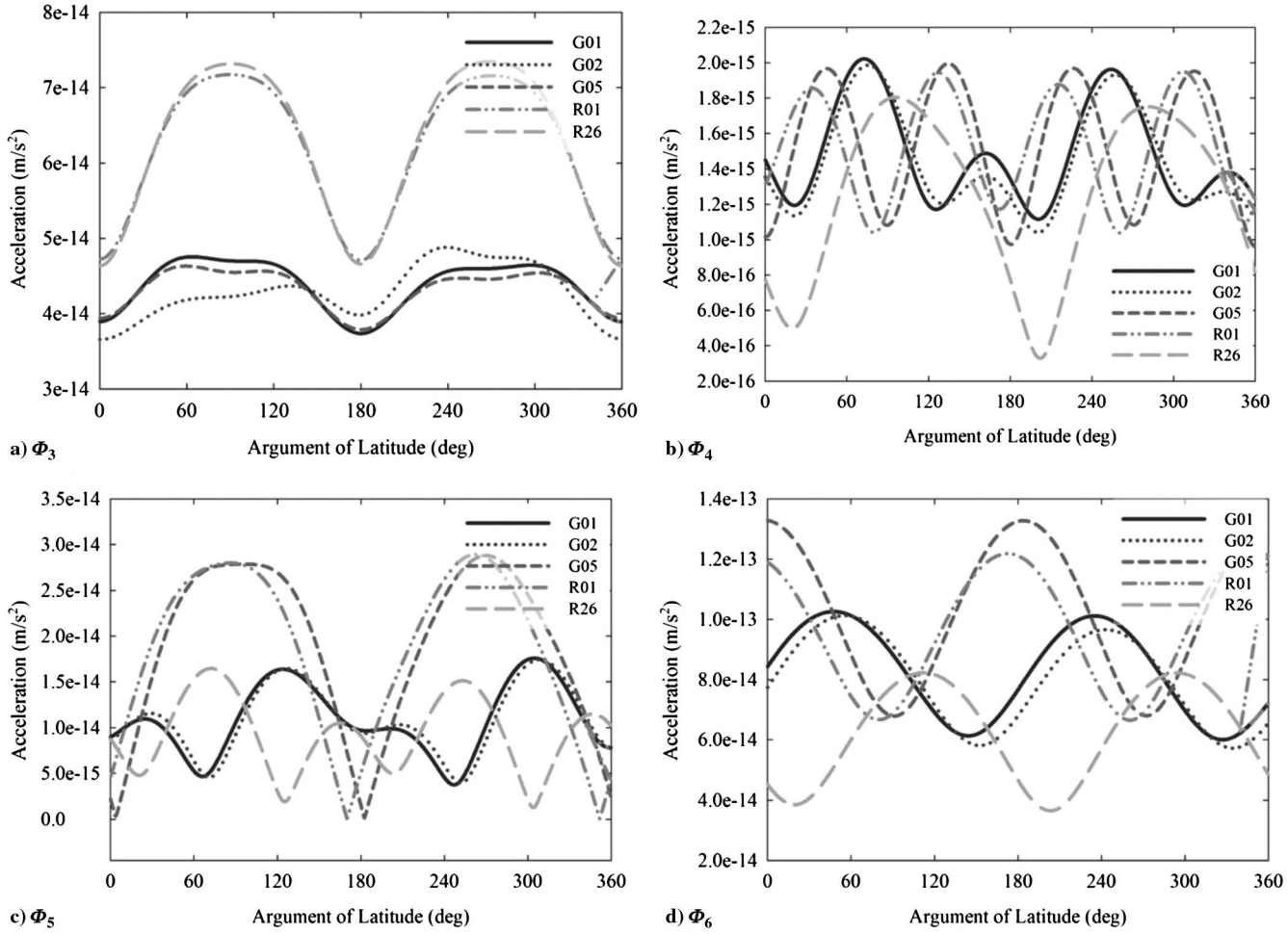

Fig. 3 Accelerations of the Φ_3 to Φ_6 terms for the various satellites.

resulting effects were expected to be analogous to the GPS case, owing to the similar levels of the PN corrections, as shown in Fig. 3. The Schwarzschild term yielded the largest position errors, which reached several meters after one week. The geodesic precession and the Lense–Thirring term were the next dominant terms, yielding maximal position differences of ∼10 cm and ∼1 cm, respectively. The position differences caused by the remaining PN corrections were under 1 mm. However, it is very important to clarify the extent to which individual PN terms affect the GPS and GLONASS orbits because precise orbit determination requires the error levels between observations and calculations to be as small as possible, especially considering the rapid advances in the measurement technology in the GNSS [1].

Table 3 Effects of the different PN corrections on the satellite position

	Maximal radial, mm	Maximal alongtrack, mm	Maximal crosstrack, mm	Maximal position, mm
Case 1 (with/without $\mathbf{\Phi}_1$)	35.38	2289.66	0.05	2289.93
Case 2 (with/without $\mathbf{\Phi}_{GP}$)	0.89	69.58	46.69	83.80
Case 3 (with/without $\mathbf{\Phi}_2$)	0.10	8.37	6.14	10.38
Case 4 (with/without $\mathbf{\Phi}_6$)	0.01	0.34	0.14	0.36
Case 5 (with/without $\mathbf{\Phi}_3$)	0.0	0.21	0.05	0.21
Case 6 (with/without $\mathbf{\Phi}_5$)	0.02	0.08	0.00	0.08
Case 7 (with/without $\mathbf{\Phi}_4$)	0.0	0.01	0.00	0.01

IV. Conclusions

Advances in atomic clocks, which are one of the key technologies in a GNSS, promote the role of the GNSS in space geodesy. Therefore, there is a growing need for more accurate modeling of the equations of motion of GNSS satellites and better measurement equations. In this study, the effects of the full set of first-order PN perturbations on the GPS and GLONASS satellites were investigated by conducting realistic orbit simulations. The Schwarzschild term had the strongest relativistic effect; the magnitude of this effect was similar to that of the perturbation due to the Earth's radiation. The geodesic procession and the Lense–Thirring effects were the next strongest ones. The position differences caused by these two PN corrections reached ∼8 cm and ∼1 cm after one week of orbit propagation, respectively. The PN corrections owing to the gravitomagnetic part of the tidal potential ($\mathbf{\Phi}_6$) were the next most dominant ones, with the acceleration on the order of 10^{-13} m/s^2. The relativistic effects owing to the Earth's quadrupole moment ($\mathbf{\Phi}_3$), the gravitoelectric part of the tidal potential ($\mathbf{\Phi}_5$), the nonlinear coupling of the monopole attracting force of the Earth, and the gravitoelectric tidal field ($\mathbf{\Phi}_4$) were on the orders of 10^{-14} and 10^{-16} m/s^2. The position differences caused by the last four PN corrections were under 1 mm after one week of orbit propagation. These corrections can be considered to be negligible at the current moment, considering the accuracy of the final orbit solutions released by the IGS. However, it is worthy to evaluate the effects of the full set of the PN corrections by conducting extensive numerical simulations to define the extent of the effects of these negligible perturbations and to prepare for their use in the future.

Appendix: Decomposed Accelerations of the First-Order PN Corrections

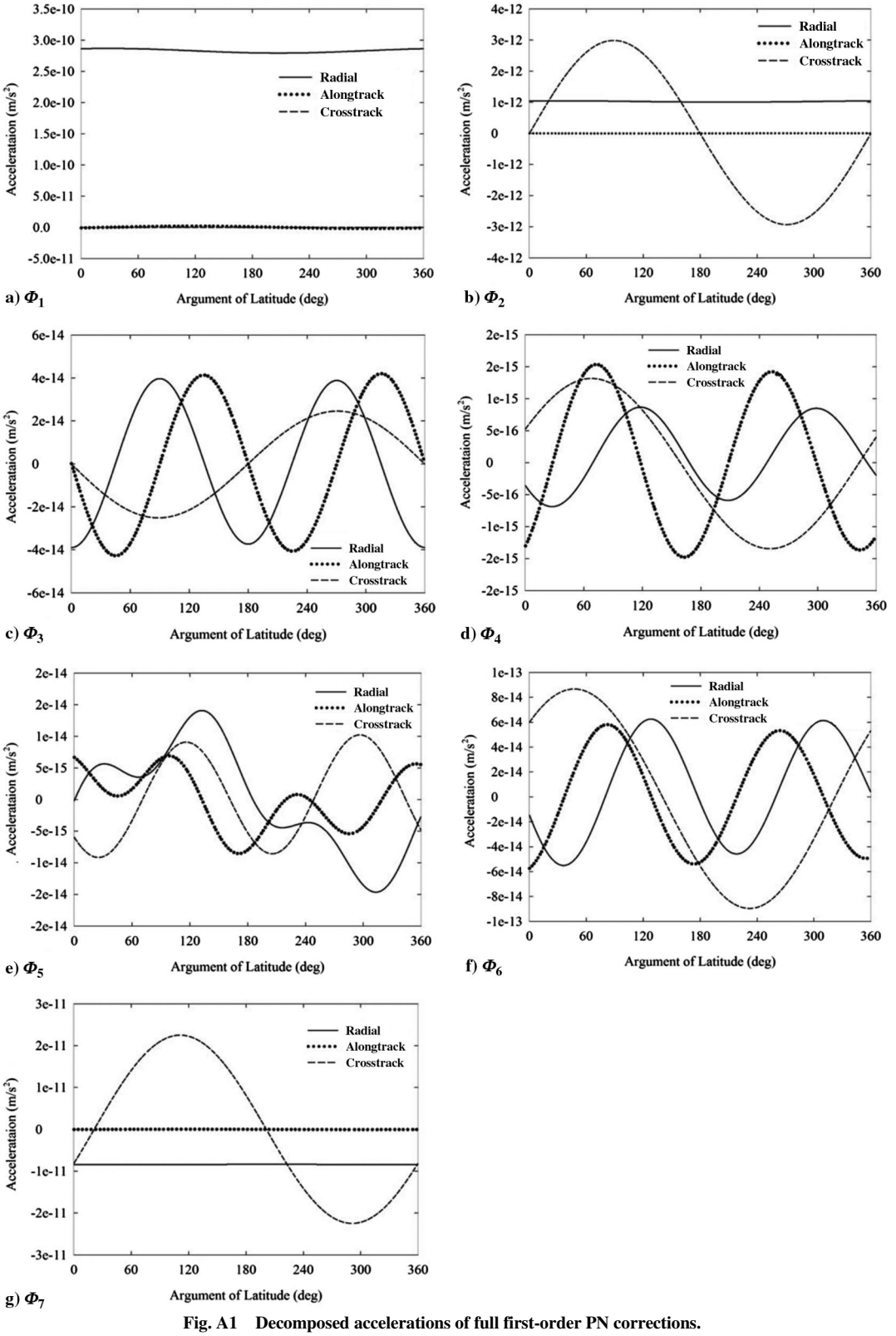

Fig. A1 Decomposed accelerations of full first-order PN corrections.

References

[1] Kopeikin, S. M., (ed.), *Frontiers in Relativistic Celestial Mechanics*, Vol. 2, Applications and Experiments, Walter de Gruyter, Berlin, 2014, Chap. 7.

[2] Ashby, N., "Relativity in the Global Positioning System," *Living Reviews in Relativity*, Vol. 6, No. 1, Jan. 2003, p. 1. doi:10.12942/lrr-2003-1

[3] McCarthy, D. D., *IERS Standards (1992)*, Central Bureau of International Earth Rotation and Reference System Service TN 13, Paris, 1992.

[4] Petit, G., and Luzum, B. (eds.), *IERS Conventions (2010)*, Central Bureau of International Earth Rotation and Reference System Service TN 36, Frankfurt am Main, Germany, 2010.

[5] Steigenberger, P., *Reprocessing of a Global GPS Network*, Deutsche Geodaetische Kommission, Munich, 2009.

[6] Hećimović, Z., "Relativistic Effects on Satellite Navigation," *Tehnicki Vjesnik*, Vol. 20, No. 1, Feb. 2013, pp. 195–203.

[7] Rodriguez-Solano, C. J., Hugentobler, U., and Steigenberger, P., "Adjustable Box-Wing Model for Solar Radiation Pressure Impacting GPS Satellites," *Advances in Space Research*, Vol. 49, No. 7, April 2012, pp. 1113–1128. doi:10.1016/j.asr.2012.01.016

[8] Roh, K.-M., Kopeikin, S. M., and Cho, J.-H., "Numerical Simulation of the Post-Newtonian Equations of Motion for the Near Earth Satellite with an Application to the LARES Satellite," *Advances in Space Research*, Vol. 58, No. 11, Dec. 2016, pp. 2255–2268. doi:10.1016/j.asr.2016.08.009

[9] Ciufolini, I., Paolozzi, A., Pavlis, E. C., Ries, J. C., Koenig, R., Matzner, R. A., Sindoni, G., and Neumayer, H., "Towards a One Percent Measurement of Frame Dragging by Spin with Satellite Laser Ranging to LAGEOS, LAGEOS 2 and LARES and GRACE Gravity Models," *Space Science Reviews*, Vol. 148, Nos. 1–4, Dec. 2009, pp. 71–104. doi:10.1007/s11214-009-9585-7

[10] Soffel, M., Klioner, S. A., Petit, G., Wolf, P., Kopeikin, S. M., Bretagnon, P., Brumberg, V. A., Capitaine, N., Damour, T., Fukushima, T., Guinot, B., Huang, T. Y., Lindegren, L., Ma, C., Nordtvedt, K., Ries, J. C., Seidelmann, P. K., Vokrouhlicky, D., Will, C. M., and Xu, C., "The IAU 2000 Resolutions for Astrometry, Celestial Mechanics, and Metrology in the Relativistic Framework: Explanatory Supplement," *Astronomical Journal*, Vol. 126, No. 6, Dec. 2003, pp. 2687–2706. doi:10.1086/378162

[11] Brumberg, V. A., and Kopejkin, S. M., "Relativistic Reference Systems and Motion of Test Bodies in the Vicinity of the Earth," *Il Nuovo Cimento B*, Vol. 103, No. 1, Jan. 1989, pp. 63–98. doi:10.1007/BF02888894

[12] Damour, T., Soffel, M., and Xu, C., "General-Relativistic Celestial Mechanics. I. Method and Definition of Reference Systems," *Physical Review D: Particles and Fields*, Vol. 43, No. 10, 1991, pp. 3273–3307. doi:10.1103/PhysRevD.43.3273

[13] Damour, T., Soffel, M., and Xu, C., "General-Relativistic Celestial Mechanics II. Translational Equations of Motion," *Physical Review D: Particles and Fields*, Vol. 45, No. 4, 1992, pp. 1017–1044. doi:10.1103/PhysRevD.45.1017

[14] Damour, T., Soffel, M., and Xu, C., "General-Relativistic Celestial Mechanics. III. Rotational Equations of Motion," *Physical Review D: Particles and Fields*, Vol. 47, No. 8, Jan. 1993, pp. 3124–3135. doi:10.1103/PhysRevD.47.3124

[15] Damour, T., Soffel, M., and Xu, C., "General-Relativistic Celestial Mechanics. IV. Theory of Satellite Motion," *Physical Review D: Particles and Fields*, Vol. 49, No. 2, 1994, pp. 618–635. doi:10.1103/PhysRevD.49.618

[16] Pavlis, N. K., Holmes, S. A., Kenyon, S. C., and Factor, J. K., "The Development and Evaluation of the Earth Gravitational Model 2008 (EGM2008)," *Journal of Geophysical Research*, Vol. 117, No. B4, April 2012, Paper B04406. doi:10.1029/2011JB008916

[17] Lyard, F., Lefevre, F., Letellier, T., and Francis, O., "Modelling the Global Ocean Tides: Modern Insights from FES2004," *Ocean Dynamics*, Vol. 56, No. 5, Dec. 2006, pp. 394–415. doi:10.1007/s10236-006-0086-x

[18] Montenbruck, O., and Gill, E., *Satellite Orbits*, Springer–Verlag, Berlin, 2011.

[19] Bowman, B. R., Tobiska, W. K., Marcos, F. A., Huang, C., Lin, C. S., and Burke, W. J., "A New Empirical Thermospheric Density Model JB2008 Using New Solar and Geomagnetic Indices," *AIAA/AAS Astrodynamics Specialist Conference and Exhibit*, AIAA Paper 2008-6438, 2008.

[20] Fienga, A., Manche, H., Laskar, J., Gastineau, M., and Verma, A. K., *INPOP New Release: INPOP13c*, IMCCE, 2014, https://www.imcce.fr/inpop.

E. G. Lightsey
Associate Editor